

SSNV197 - Triaxial drained with the law of Hujeux

Summary

One is carried out *triaxial calculation in pure mechanics* (equivalent under drained hydraulic conditions) with *the law of Hujeux*. The calculated solutions are compared with results resulting from the code finite elements GEFDYN of the Central School Paris. The first four modelings of this test are carried out with an assumption small deformations (DEFORMATION=' PETIT '):

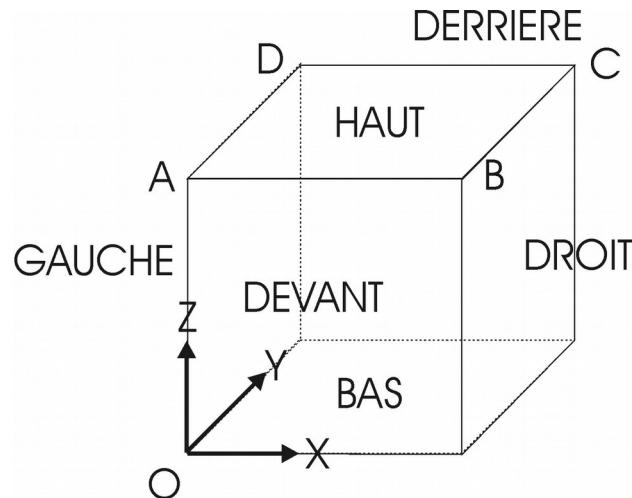
- one préconsolide the test-tube until 50 kPa (surconsolidé state);
- one préconsolide the test-tube until 100 kPa (fairly consolidated state);
- one préconsolide the test-tube until 200 kPa (normally consolidated state);
- one préconsolide the test-tube until 100 kPa (normally consolidated state), but one uses a sample with surfaces slip (related to the mechanisms déviatoires) tilted of 45° compared to the vertical;

The three following tests take again the same tests with a kinematics great deformations provided by operator GDEF_LOG: (DEFORMATION=' GDEF_LOG '):

- one préconsolide the test-tube until 50 kPa (surconsolidé state);
- one préconsolide the test-tube until 100 kPa (fairly consolidated state);
- one préconsolide the test-tube until 200 kPa (normally consolidated state);

1 Problem of reference

1.1 Geometry



The triaxial compression test is carried out on only one isoparametric finite element of cubic form *CUB8*. The length of each edge is worth 1. The various facets of this cube are named groups of meshes *HAUT*, *BAS*, *DEVANT*, *DERRIERE*, *DROIT* and *GAUCHE*. The group of meshes *SYM* contains the groups of meshes in addition *BAS*, *DEVANT* and *GAUCHE*; the group of meshes *COTE* groups of meshes *DERRIERE* and *DROIT*.

1.2 Material properties

The elastic properties are:

- isotropic module of compressibility: $K = 516200 \text{ kPa}$
- modulus of rigidity: $\mu = 238200 \text{ kPa}$

The unelastic properties (Hujeux) are:

- power of the non-linear elastic law: $n_e = 0.4$
- $\beta = 24$
- $d = 2.5$
- $b = 0.2$
- angle of friction: $\varphi = 33^\circ$
- angle of dilatancy: $\psi = 33^\circ$
- critical pressure: $P_{c0} = -1000 \text{ kPa}$
- pressure of reference: $P_{ref} = -1000 \text{ kPa}$
- elastic ray of the isotropic mechanism: $r_{\text{éla}}^s = 0.001$
- elastic ray of the mechanism déviatoire: $r_{\text{éla}}^d = 0.005$
- $a_{\text{mon}} = 0.0001$
- $a_{\text{cyc}} = 0.008$
- $c_{\text{mon}} = 0.2$
- $c_{\text{cyc}} = 0.1$
- $r_{\text{hys}} = 0.05$
- $r_{\text{mob}} = 0.9$
- $x_m = 1$
- $\text{dila} = 1$

1.3 Boundary conditions and loadings

A triaxial compression test consists in imposing on the test-tube a vertical radial force all while keeping the side pressure constant. It can be drained (the pore water pressure of fluid does not vary during the test) or not-drained (one turns off the tap: the pore water pressure of fluid evolves in the sample). One is interested here in the case drained, simpler, because not utilizing the influence of the pore water pressure of the fluid and *modélisable of this fact by a pure mechanical calculation*.

In the model considered, the cubic element represents a eighth of the sample. The limiting conditions are thus the following ones:

- Conditions of symmetry:
 - $u_z = 0$ on the group of mesh *BAS*
 - $u_x = 0$ on the group of mesh *GAUCHE*
 - $u_y = 0$ on the group of mesh *DEVANT*
- Conditions of side pressure:
 - $P_n = 1$ on the group of mesh *COTE*
- Conditions of loading:
 - $P_n = 1$ on the group of mesh *HAUT* (phase 1)
 - $u_z = -1$ on the group of mesh *HAUT* (phase 2)

The loading is carried out in two phases:

- isotropic loading enters $t = -2$ and $t = 0$ where pressure on the groups of meshes *COTE* and *HIGH* varies between $p = 0$ and $p = p_c$ (isotropic pressure of preconsolidation). In modelings A, B and C, the value of p_c is respectively of 50, 100, 200 kPa ;
- displacement imposed on the group of meshes *HAUT* and variable enters $t = 0$ and $t = 10$ of $u_z = 0$ and $u_z = -0.2$ (total vertical deformation of 20%).

1.4 Results

The solutions post-are treated with the point *C*, in terms of equivalent constraint Q , of total voluminal deformation ε_v and of coefficients of isotropic work hardening $(r_{ela}^{s,m} + r_{iso}^m)$ and déviatoire $(r_{ela}^{d,m} + r_{dev}^m)$, according to the evolution of the axial deformation ε_{zz}

The validation is carried out by comparison with solutions GEFDYN provided by the Central School Paris.

For modelings proposing the approach great deformations with operator GDEF_LOG, one considers the deformation logarithmic curve $\underline{E} = 1/2 \log(I + 2 \underline{\Delta})$, with $\underline{\Delta}$ the tensor of Green-Lagrange. The voluminal deformation in this case is directly obtained starting from the determinant of the gradient of deformation, $J = \det(F)$.

2 Modeling A

2.1 Characteristics of modeling

Modeling A is *three-dimensional and non-linear statics*.

One carries out initially one *elastic preconsolidation (ELAS)* sample until $p_c = 50\text{kPa}$ (1^{ère} phase of calculation). This preconsolidation takes place in 1 pas de time enters $t = -2$ and $t = 0$.

The vertical displacement imposed on the higher facet varies between 0. and -0.2 (2^{ème} phase of calculation) in 100 pas de time enters $t = 0$ and $t = 10$. At the time of this second phase, one activates the automatic subdivision of the step of time to manage the situations of nonconvergence of local integration.

In the integration of the equilibrium equations, one asks for a reactualization of the tangent matrix, which is provided by the routines of the law of Hujeux and accelerates convergence appreciably. One also asks for the subdivision of the step of time (order `DEFI_LIST_INST`) to treat the situations of failure of local integration due to too large increments of loading. **This functionality is largely recommended.**

2.2 Sizes tested and results

2.2.1 Values tested

The solutions are calculated at the point C and compared with references GEFDYN. They are given in terms of equivalent constraint Q , of total voluminal deformation ε_V and of coefficients of isotropic work hardening $(r_{ela}^{iso,m} + r_{iso}^m)$ and déviatoire $(r_{ela}^{d,m} + r_{dev}^m)$, and recapitulated in the following tables:

$$Q = \sqrt{\frac{1}{2} \underline{s} : \underline{s}} \text{ [Pa]}$$

ε_{zz}	Code_Aster	GEFDYN	relative error
-1%	115523.	117640.	-1,799%
-2%	155466.	157072.	-1,022%
-5%	199986.	200850.	-0,430%
-10%	206823.	207649.	-0,398%
-20%	184853.	185854.	-0,539%

$$\varepsilon_V = \text{trace}(\varepsilon)$$

ε_{zz}	Code_Aster	GEFDYN	relative error
-1%	-3.78E-3	-3.82E-3	-1,125%
-2%	-4,34E-003	-4.34E-3	-0,051%
-10%	1.09E-2	1.07E-2	1,917%
-20%	3.237E-2	3.191E-2	1,433%

$$\left(r_{ela}^{d,m} + r_{dev}^m \right)$$

ξ_{zz}	Code_Aster	GEFDYN	relative error
-1%	0,673	0,679	-0,904%
-2%	0,781	0,784	-0,406%
-5%	0,887	0,888	-0,107%
-10%	0,937	0,937	0,004%
-20%	0,966	0,967	-0,054%

$$\left(r_{ela}^{iso,m} + r_{iso}^m \right)$$

ξ_{zz}	Code_Aster	GEFDYN	relative error
-1%	0.0325	0.0328	-0,900%
-2%	0.0370	0.0372	-0,663%
-5%	0.0466	0.0467	-0,296%
-10%	0.0624	0.0623	0,085%
-20%	0.0979	0.0973	0,576%

2.2.2 Comments

The difference between the two codes is very weak (lower than 2%).

3 Modeling B

3.1 Characteristics of modeling

Modeling B is *three-dimensional* and *non-linear statics*.

One carries out initially one *elastic preconsolidation* (*ELAS*) sample until $p_c = 100 \text{ kPa}$ (1^{era} phase of calculation). This preconsolidation takes place in 1 pas de time enters $t = -2$ and $t = 0$.

The vertical displacement imposed on the higher facet varies between 0. and -0.2 (2^{eme} phase of calculation) in 100 pas de time enters $t = 0$ and $t = 10$. At the time of this second phase, one activates the automatic subdivision of the step of time to manage the situations of nonconvergence of local integration. In the integration of the equilibrium equations, one asks for a reactualization of the tangent matrix, which is provided by the routines of the law of Hujeux and accelerates convergence appreciably. One also asks for the subdivision of the step of time (order `DEFI_LIST_INST`) to treat the situations of failure of local integration due to too large increments of loading. **This functionality is largely recommended.**

3.2 Sizes tested and results

3.2.1 Values tested

The solutions are calculated at the point *C* and compared with references GEFDYN. They are given in terms of equivalent constraint Q , of total voluminal deformation ε_v and of coefficients of isotropic work hardening ($r_{ela}^{iso,m} + r_{iso}^m$) and déviatoire ($r_{ela}^{d,m} + r_{dev}^m$), and recapitulated in the following tables:

$$Q = \sqrt{\frac{1}{2} \underline{\underline{s}} : \underline{\underline{s}}} \text{ [Pa]}$$

ε_{zz}	Code_Aster	GEFDYN	relative error
-1%	188768.	191799.	-1,580%
-2%	253219.	255501.	-0,893%
-5%	329638.	330404.	-0,232%
-10%	355436.	355895.	-0,129%
-20%	340728.	341220.	-0,144%

$$\varepsilon_v = \text{trace}(\varepsilon)$$

ε_{zz}	Code_Aster	GEFDYN	relative error
-1%	-5.47E-3	-5.53E-3	-1,086%
-2%	-7.128E-3	-7.15E-3	-0,314%
-5%	-6.684E-3	-6.64E-3	0,660%
-10%	-8.227E-4	-8.22E-4	0,083%
-20%	1.261E-2	1.25E-2	0,905%

$$(r_{ela}^{d,m} + r_{dev}^m)$$

ε_{zz}	Code_Aster	GEFDYN	relative error
-1%	0,659	0,665	-0,879%
-2%	0,772	0,775	-0,431%
-5%	0,882	0,883	-0,115%
-10%	0,934	0,934	0,010%
-20%	0,965	0,965	0,010%

$$(r_{ela}^{iso,m} + r_{iso}^m)$$

ε_{zz}	Code_Aster	GEFDYN	relative error
-1%	0.0575	0.0578	-0,466%
-2%	0.0627	0.0630	-0,471%
-5%	0.0723	0.0725	-0,286%
-10%	0.0867	0.0868	-0,132%
-20%	0,169	0,117	-0,054%

3.2.2 Comments

The relative error is higher when the values tested are lower, which is not abnormal. Ultimately, the difference between the two codes is very reasonable.

4 Modeling C

4.1 Characteristics of modeling

Modeling *C* is *three-dimensional* and *non-linear statics*.

One carries out initially one *elastic preconsolidation* (*ELAS*) sample until $p_c = 200 \text{ kPa}$ (1^{era} phase of calculation). This preconsolidation takes place in 1 pas de time enters $t = -2$ and $t = 0$.

The vertical displacement imposed on the higher facet varies between 0 and -0.2 (2^{ème} phase of calculation) in 100 pas de time enters $t = 0$ and $t = 10$. At the time of this second phase, one activates the automatic subdivision of the step of time to manage the situations of nonconvergence of local integration. In the integration of the equilibrium equations, one asks for a reactualization of the tangent matrix, which is provided by the routines of the law of Hujeux and accelerates convergence appreciably. One also asks for the subdivision of the step of time (order `DEFI_LIST_INST`) to treat the situations of failure of local integration due to too large increments of loading. **This functionality is largely recommended.**

4.2 Sizes tested and results

4.2.1 Values tested

The solutions are calculated at the point *C* and compared with references GEFDYN. They are given in terms of equivalent constraint Q , of total voluminal deformation ε_V and of coefficients of isotropic work hardening $(r_{ela}^{iso,m} + r_{iso}^m)$ and déviatoire $(r_{ela}^{d,m} + r_{dev}^m)$, and recapitulated in the following tables:

$$Q = \sqrt{\frac{1}{2} \underline{\underline{\varepsilon}} : \underline{\underline{\varepsilon}}} \text{ [Pa]}$$

ε_{zz}	Code_Aster	GEFDYN	relative error
-1%	306905.	311459.	-1,462%
-2%	413405.	416832.	-0,822%
-5%	543741.	545338.	-0,293%
-10%	605206.	605666.	-0,076%
-20%	616663.	616946.	-0,046%

$$\varepsilon_V = \text{trace}(\varepsilon)$$

ε_{zz}	Code_Aster	GEFDYN	relative error
-1%	-7.389E-3	-7.47E-3	-1,086%
-2%	-1.001E-2	-1.005E-2	-0,387%
-5%	-1.229E-2	-1.227E-2	0,175%
-10%	-1.096E-2	-1.092E-2	0,367%
-20%	-4.88E-3	-4.88E-3	-0,007%

$$\left(r_{ela}^{d,m} + r_{dev}^m \right)$$

ξ_{zz}	Code_Aster	GEFDYN	relative error
-1%	0,642	0,648	-0,939%
-2%	0,761	0,765	-0,488%
-5%	0,877	0,878	-0,130%
-10%	0,931	0,932	-0,087%
-20%	0,964	0,964	-0,031%

$$\left(r_{ela}^{iso,m} + r_{iso}^m \right)$$

ξ_{zz}	Code_Aster	GEFDYN	relative error
-1%	0,102	0,102	0,112%
-2%	0,107	0,108	-0,532%
-5%	0,115	0,115	0,116%
-10%	0,125	0,126	-0,450%
-20%	0,147	0,147	-0,301%

4.2.2 Comments

The relative error is higher when the values tested are lower. Ultimately, the difference between the two codes is very reasonable.

5 Modeling D

5.1 Characteristics of modeling

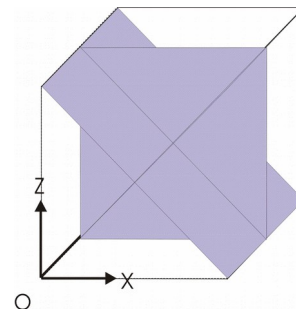
The goal of this modeling is to test the functionality of reorientation of the local reference mark defining the three slip surfaces related to the mechanisms déviatoires of the law of Hujeux. This reorientation is carried out using the operator `AFFE_CARA_ELEM` → `SOLID MASS`.

Modeling D is *three-dimensional* and *non-linear statics*.

One carries out initially one *elastic preconsolidation* (*ELAS*) sample until $p_c = 100 \text{ kPa}$ (1^{ère} phase of calculation). This preconsolidation takes place in 1 pas de time enters $t = -2$ and $t = 0$.

The vertical displacement imposed on the higher facet varies between 0. and -0.2 (2^{ème} phase of calculation) in 100 pas de time enters $t = 0$ and $t = 10$. At the time of this second phase, one activates the automatic subdivision of the step of time to manage the situations of nonconvergence of local integration.

One tests the reorientation of the slip surfaces defined by a rotation of the reference mark of 45° around the axis (*OZ*). This reorientation is defined by `AFFE_CARA_ELEM` → `SOLID MASS`.



The object is charged `CARAEEL` laying down the direction of the local reference mark on which the slip surfaces of the law of Hujeux will be defined. In the integration of the equilibrium equations, one asks for a reactualization of the tangent matrix, which is provided by the routines of the law of Hujeux and accelerates convergence appreciably. One also asks for the subdivision of the step of time (order `DEFI_LIST_INST`) to treat the situations of failure of local integration due to too large increments of loading. **This functionality is largely recommended.**

5.2 Sizes tested and results of modeling D

5.2.1 Values tested

The solutions are calculated at the point *C* and compared with an identical calculation carried out (with Code_Aster) on a sample turned beforehand of 45° . They are given in terms of equivalent constraint Q , of total voluminal deformation ε_v and of coefficients of isotropic work hardening $(r_{ela}^{iso,m} + r_{iso}^m)$ and déviatoire $(r_{ela}^{d,m} + r_{dev}^m)$, and recapitulated in the following tables:

$$Q = \sqrt{\frac{1}{2} \underline{\underline{s}} : \underline{\underline{s}}} \quad [Pa]$$

ε_{zz}	Code_Aster	GEFDYN	relative error
-2%	148396	148396	0,0002%
-4%	176513	176513	0,006%
-6%	185559	185554	0,002%
-8%	187683	187681	0,001%
-10%	186806	186804	0,001%

$$\varepsilon_V = \text{trace}(\varepsilon)$$

ε_{zz}	Code_Aster	GEFDYN	relative error
-2%	-7,40E-3	-7,40E-3	0,001%
-4%	-6,72E-3	-6,72E-3	0,016%
-6%	-4,36E-3	-4,36E-3	-0,001%
-8%	-1,45E-3	-1,45E-3	-0,013%
-10%	1,63E-3	1,63E-3	0,018%

$$(r_{ela}^{d,m} + r_{dev}^m)$$

ε_{zz}	Code_Aster	GEFDYN	relative error
-2%	0,565	0,565	-0,062%
-4%	0,630	0,630	0,008%
-6%	0,654	0,654	0,073%
-8%	0,666	0,666	-0,035%
-10%	0,671	0,671	0,054%

$$(r_{ela}^{iso,m} + r_{iso}^m)$$

ε_{zz}	Code_Aster	GEFDYN	relative error
-2%	0,067	0,067	-0,564%
-4%	0,074	0,074	0,140%
-6%	0,081	0,081	-0,499%
-8%	0,087	0,087	-0,038%
-10%	0,093	0,093	0,421%

5.2.2 Comments

The relative error is always very weak, which is normal, since it is ultimately exactly the same calculation.

6 Modeling E

6.1 Characteristics of modeling

Modeling E is *three-dimensional* and *non-linear statics*.

One carries out initially one *elastic preconsolidation (ELAS)* sample until $p_c = 50\text{kPa}$ (1^{ère} phase of calculation). This preconsolidation takes place in 1 pas de time enters $t = -2$ and $t = 0$.

The vertical displacement imposed on the higher facet varies between 0. and -0.2 (2^{ème} phase of calculation) in 100 pas de time enters $t = 0$ and $t = 10$. Modeling considers one kinematics great deformations with operator GDEF_LOG (DEORMATION=' GDEF_LOG').

In the integration of the equilibrium equations, one asks for a reactualization of the tangent matrix, which is provided by the routines of the law of Hujeux and accelerates convergence appreciably. One also asks for the subdivision of the step of time (order DEFI_LIST_INST) to treat the situations of failure of local integration due to too large increments of loading. **This functionality is largely recommended.**

6.2 Sizes tested and results

6.2.1 Values tested

The solutions are calculated at the point C and compared at the same time with the results of modeling A and the values of reference of GEFDYN. They are given in terms of equivalent constraint Q , of total voluminal deformation $\varepsilon_v / J = \det(\underline{E})$ and of coefficients of isotropic work hardening ($r_{ela}^{iso,m} + r_{iso}^m$) and déviatoire ($r_{ela}^{d,m} + r_{dev}^m$), and recapitulated in the following tables:

$$Q = \sqrt{\frac{1}{2} \underline{s} : \underline{s}} \text{ [Pa]}$$

ε_{zz}, E_{zz}	Code_Aster (SMALL DEFORMATION= ')	Code_Aster (DEFORMATION= ' GDEF_LOG)	relative error	GEFDYN	relative error
-1%	115523.	115620.	0,104%	117640.	1,717%
-2%	155466.	155603.	0,097%	157072.	0,935%
-5%	199986.	199911.	0,033%	200850.	0,468%
-10%	206823.	206191.	0,305%	207649.	0,702%
-20%	184853.	183693.	0,628%	185854.	1,162%

$$\varepsilon_v = \text{trace}(\underline{\varepsilon}), \quad J = \det(\underline{E})$$

ε_{zz}, E_{zz}	Code_Aster (SMALL DEFORMATION= ')	Code_Aster (DEFORMATION= ' GDEF_LOG)	relative error	GEFDYN	relative error
-1%	-3.78E-3	-0.00374	0,825%	-3.82E-3	1,946%
-2%	-4,34E-003	-0.00429	1,067%	-4.34E-3	1,109%
-10%	1.09E-2	0.01084	0,573%	1.07E-2	1,319%

-20%	3.237E-2	0.03226	0,337%	3.191E-2	1,086%
------	----------	---------	--------	----------	--------

$$(r_{ela}^{d,m} + r_{dev}^m)$$

ε_{zz}, E_{zz}	Code_Aster (SMALL DEFORMATION='')	Code_Aster (DEFORMATION= ' GDEF_LOG)	relative error	GEFDYN	relative error
-1%	0,673	0,673	5.45E-03%	0,679	0,909%
-2%	0,781	0,781	5.23E-03%	0,784	0,416%
-5%	0,887	0,887	0.01258%	0,888	0,121%
-10%	0,937	0,937	0.00915%	0,937	6.51E-03%
-20%	0,966	0,966	6.58E-03%	0,967	0,061%

$$(r_{ela}^{iso,m} + r_{iso}^m)$$

ε_{zz}, E_{zz}	Code_Aster (SMALL DEFORMATION='')	Code_Aster (DEFORMATION= ' GDEF_LOG)	relative error	GEFDYN	relative error
-1%	0.0325	0.0324	0,276%	0.0328	1,181%
-2%	0.0370	0.0368	0,296%	0.0372	0,962%
-5%	0.0466	0.0465	4.28E-03%	0.0467	0,305%
-10%	0.0624	0.0627	0,629%	0.0623	0,710%
-20%	0.0979	0.0992	1,396%	0.0973	1,976%

6.2.2 Comments

It is observed that the result of integration in great deformations with operator GDEF_LOG allows to reproduce, with enriched kinematics, the behavior prescribes by the law of behavior (variation to the maximum about 1% for the voluminal deformations). See the Figures 5 and 6.

7 Modeling F

7.1 Characteristics of modeling

Modeling B is *three-dimensional* and *non-linear statics*.

One carries out initially one *elastic preconsolidation* (*ELAS*) sample until $p_c = 100 \text{ kPa}$ (1^{era} phase of calculation). This preconsolidation takes place in 1 pas de time enters $t = -2$ and $t = 0$.

The vertical displacement imposed on the higher facet varies between 0. and -0.2 (2^{eme} phase of calculation) in 100 pas de time enters $t = 0$ and $t = 10$. Modeling considers one kinematics great deformations with operator GDEF_LOG (DEORMATION=' GDEF_LOG').

In the integration of the equilibrium equations, one asks for a reactualization of the tangent matrix, which is provided by the routines of the law of Hujeux and accelerates convergence appreciably. One also asks for the subdivision of the step of time (order DEFI_LIST_INST) to treat the situations of failure of local integration due to too large increments of loading. **This functionality is largely recommended**.

7.2 Sizes tested and results

7.2.1 Values tested

The solutions are calculated at the point *C* and compared at the same time with the results of modeling B and the values of reference of GEFDYN. They are given in terms of equivalent constraint Q , of total voluminal deformation $\varepsilon_v / J = \det(\underline{\underline{E}})$ and of coefficients of isotropic work hardening ($r_{ela}^{iso,m} + r_{iso}^m$) and déviatoire ($r_{ela}^{d,m} + r_{dev}^m$), and recapitulated in the following tables:

$$Q = \sqrt{\frac{1}{2} \underline{\underline{s}} : \underline{\underline{s}}} \text{ [Pa]}$$

ε_{zz}, E_{zz}	Code_Aster (SMALL DEFORMATION= ')	Code_Aster (DEFORMATION= ' GDEF_LOG)	relative error	GEFDYN	relative error
-1%	188768.	189073.	0,304%	191799.	1,421%
-2%	253219.	253669.	0,233%	255501.	0,717%
-5%	329638.	330053.	0,151%	330404.	0,106%
-10%	355436.	355331.	0,020%	355895.	0,158%
-20%	340728.	339806.	0,271%	341220.	0,414%

$$\varepsilon_V = \text{trace}(\underline{\varepsilon}), \quad J = \det(\underline{F})$$

ε_{zz}, E_{zz}	Code_Aster (SMALL DEFORMATION= ')	Code_Aster (DEFORMATION= ' GDEF_LOG)	relative error	GEFDYN	relative error
-1%	-5.47E-3	-0.00540	1,172%	-5.53E-3	2,340%
-2%	-7.128E-3	-0.00702	1,521%	-7.15E-3	1,831%
-5%	-6.684E-3	-0.00655	2,029%	-6.64E-3	1,338%
-10%	-8.227E-4	-0.00077	7,481%	-8.22E-4	6,775%
-20%	1.261E-2	0.01248	1,026%	1.25E-2	0,189%

$$(r_{ela}^{d,m} + r_{dev}^m)$$

ε_{zz}, E_{zz}	Code_Aster (SMALL DEFORMATION=')	Code_Aster (DEFORMATION= ' GDEF_LOG)	relative error	GEFDYN	relative error
-1%	0,659	0,659	0,108%	0,665	0,853%
-2%	0,772	0,772	0,042%	0,775	0,418%
-5%	0,882	0,882	0,010%	0,883	0,117%
-10%	0,934	0,934	2.03E-03%	0,934	5.24E-03%
-20%	0,965	0,965	1.36E-03%	0,965	5.78E-03%

$$(r_{ela}^{iso,m} + r_{iso}^m)$$

ε_{zz}, E_{zz}	Code_Aster (SMALL DEFORMATION=')	Code_Aster (DEFORMATION= ' GDEF_LOG)	relative error	GEFDYN	relative error
-1%	0.0575	0.0573	0,313%	0.0578	0,820%
-2%	0.0627	0.0624	0,407%	0.0630	0,901%
-5%	0.0723	0.0721	0,314%	0.0725	0,619%
-10%	0.0867	0.0867	0,060%	0.0868	0,090%
-20%	0,169	0,118	0,624%	0,117	0,552%

7.2.2 Comments

It is observed that the result of integration in great deformations with operator GDEF_LOG allows to reproduce, with enriched kinematics, the behavior prescribes by the law of behavior. In this case a more important variation is observed for high deformations (variation to the maximum about 10%). See the Figures 5 and 6.

8 Modeling G

8.1 Characteristics of modeling

Modeling C is *three-dimensional* and *non-linear statics*.

One carries out initially one *elastic preconsolidation* ($ELAS$) sample until $p_c = 200 \text{ kPa}$ (1^{er}a phase of calculation). This preconsolidation takes place in 1 pas de time enters $t = -2$ and $t = 0$.

The vertical displacement imposed on the higher facet varies between 0 and -0.2 (2^{ème} phase of calculation) in 100 pas de time enters $t = 0$ and $t = 10$. Modeling considers one kinematics great deformations with operator $GDEF_LOG$ (DEORMATION=' GDEF_LOG').

In the integration of the equilibrium equations, one asks for a reactualization of the tangent matrix, which is provided by the routines of the law of Hujeux and accelerates convergence appreciably. One also asks for the subdivision of the step of time (order $DEFI_LIST_INST$) to treat the situations of failure of local integration due to too large increments of loading. **This functionality is largely recommended.**

8.2 Sizes tested and results

8.2.1 Values tested

The solutions are calculated at the point C and compared at the same time with the results of modeling C and the values of reference of GEFDYN. They are given in terms of equivalent constraint Q , of total voluminal deformation $\varepsilon_v / J = \det(\underline{\underline{F}})$ and of coefficients of isotropic work hardening ($r_{ela}^{iso,m} + r_{iso}^m$) and déviatoire ($r_{ela}^{d,m} + r_{dev}^m$), and recapitulated in the following tables:

$$Q = \sqrt{\frac{1}{2} \underline{\underline{\varepsilon}} : \underline{\underline{\varepsilon}}} \text{ [Pa]}$$

ε_{zz}, E_{zz}	Code_Aster (SMALL DEFORMATION= ')	Code_Aster (DEFORMATION= ' GDEF_LOG)	relative error	GEFDYN	relative error
-1%	306905.	307810.	0,995%	311459.	1,171%
-2%	413405.	414492.	0,610%	416832.	0,561%
-5%	543741.	545019.	0,335%	545338.	0,058%
-10%	605206.	606137	0,179%	605666.	0,078%
-20%	616663.	616650.	0,010%	616946.	0,048%

$$\varepsilon_V = \text{trace}(\underline{\varepsilon}), \quad J = \det(\underline{F})$$

ε_{zz}, E_{zz}	Code_Aster (SMALL DEFORMATION= ')	Code_Aster (DEFORMATION= ' GDEF_LOG)	relative error	GEFDYN	relative error
-1%	-7.389E-3	-0.00725	1,404%	-7.47E-3	2,934%
-2%	-1.001E-2	-0.00979	2,055%	-1.005E-2	2,572%
-5%	-1.229E-2	-0.01197	2,730%	-1.227E-2	2,447%
-10%	-1.096E-2	-0.01063	3,263%	-1.092E-2	2,673%
-20%	-4.88E-3	-0.00467	4,941%	-4.88E-3	4,365%

$$(r_{ela}^{d,m} + r_{dev}^m)$$

ε_{zz}, E_{zz}	Code_Aster (SMALL DEFORMATION=')	Code_Aster (DEFORMATION= ' GDEF_LOG)	relative error	GEFDYN	relative error
-1%	0,642	0,643	0,536%	0,648	0,835%
-2%	0,761	0,762	0,245%	0,765	0,438%
-5%	0,877	0,877	0,074%	0,878	0,113%
-10%	0,931	0,931	0,027%	0,932	0,083%
-20%	0,964	0,964	7.82E-03%	0,964	0,031%

$$(r_{ela}^{iso,m} + r_{iso}^m)$$

ε_{zz}, E_{zz}	Code_Aster (SMALL DEFORMATION=')	Code_Aster (DEFORMATION= ' GDEF_LOG)	relative error	GEFDYN	relative error
-1%	0,102	0,102	0,218%	0,102	0,263%
-2%	0,107	0,107	0,376%	0,108	1,016%
-5%	0,115	0,115	0,438%	0,115	0,405%
-10%	0,125	0,125	0,282%	0,126	0,805%
-20%	0,147	0,147	0,069%	0,147	0,298%

8.2.2 Comments

It is observed that the result of integration in great deformations with operator GDEF_LOG allows to reproduce, with enriched kinematics, the behavior prescribes by the law of behavior. In this case a more important variation is observed for high deformations (variation to the maximum about 5%). See the Figures 5 and 6.

9 Summary of the results

One represents in the following curves the various comparisons between Code_Aster and Xloi (calculation programme of law of behavior, not finite elements, on a material point. The law of Hujeux which is implemented there is identical to that which is in GEFDYN), in terms of constraint déviatoire (Figure 1), of total voluminal deformation (Figure 2) and of coefficients of work hardening déviatoires (Figure 3) and isotropic (Figure 4).

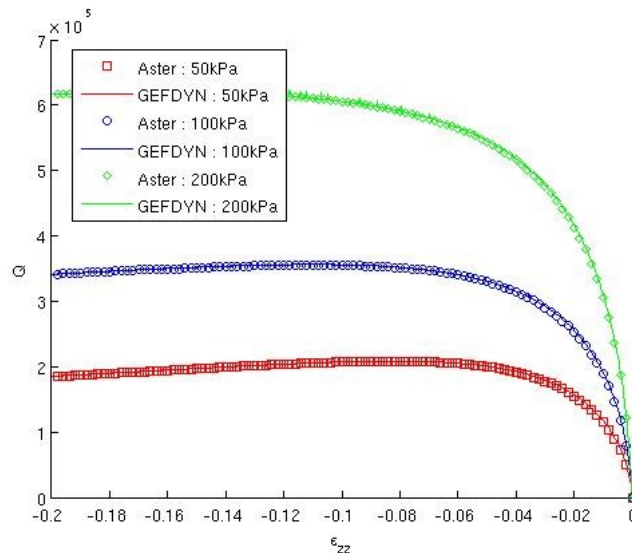


Figure 1 : Equivalent constraint (noted “ Q ”) according to the axial deformation: comparison enters the solutions Code_Aster and Xloi, for the pressures of consolidation of 50 , 100 and 200kPa .

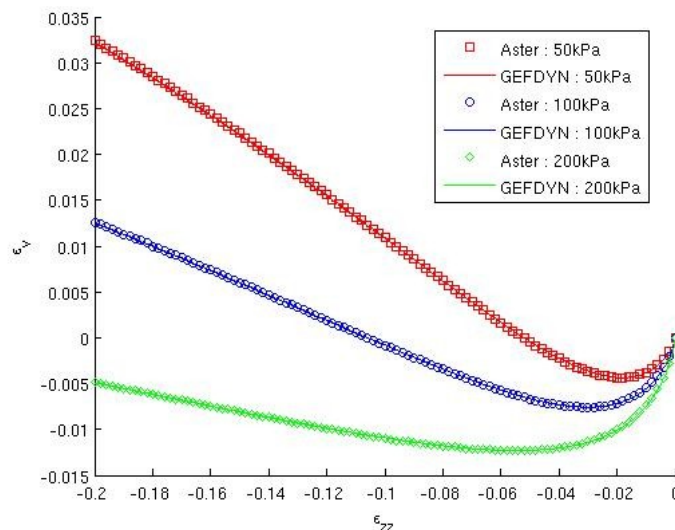


Figure 2 : Total voluminal deformation (noted “ $EPSv$ ”) according to the axial deformation: comparison enters the Code_Aster solutions and Xloi, for the pressures of consolidation of 50 , 100 and 200kPa .

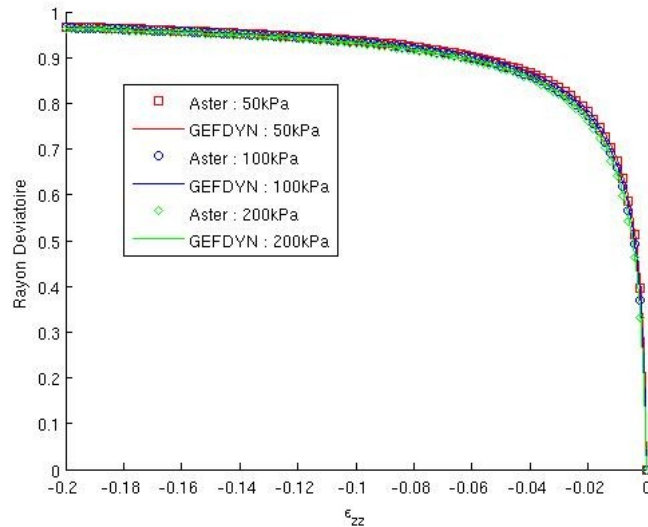


Figure 3 : ray déviatoire according to the axial deformation: comparison enters the solutions Code_Aster and Xloi, for the pressures of consolidation of 50 , 100 and 200kPa .

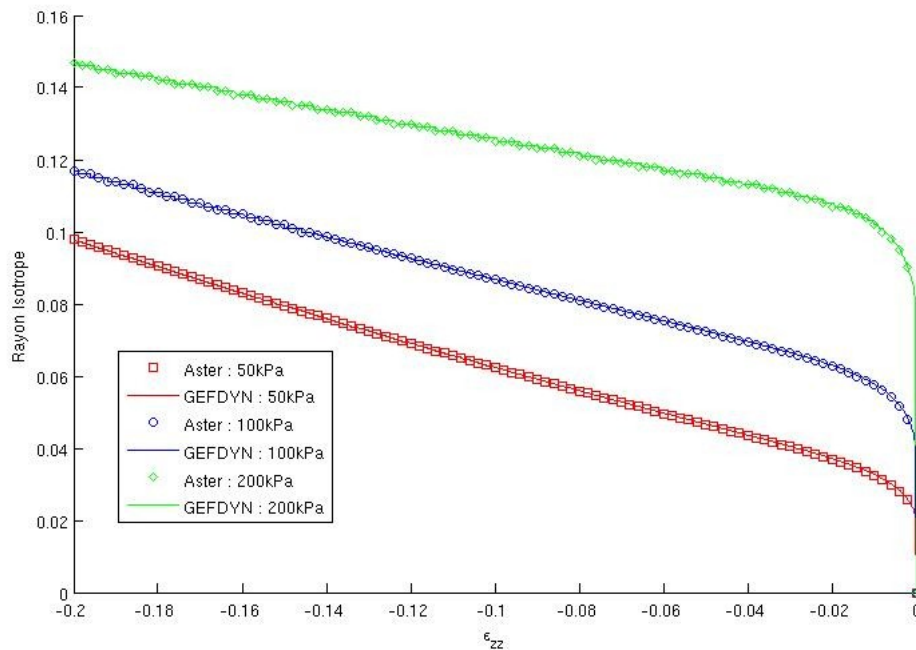


Figure 4: isotropic ray according to the axial deformation: comparison enters the solutions Code_Aster and Xloi, for the pressures of consolidation of 50 , 100 and 200kPa .

One represents in the following curves the comparisons between the results with a modeling small deformations and great deformations in Code_Aster. The Figure 5 watch the evolution of the deviatoric constraints and a comparison of the voluminal deformations is presented in Figure 6.

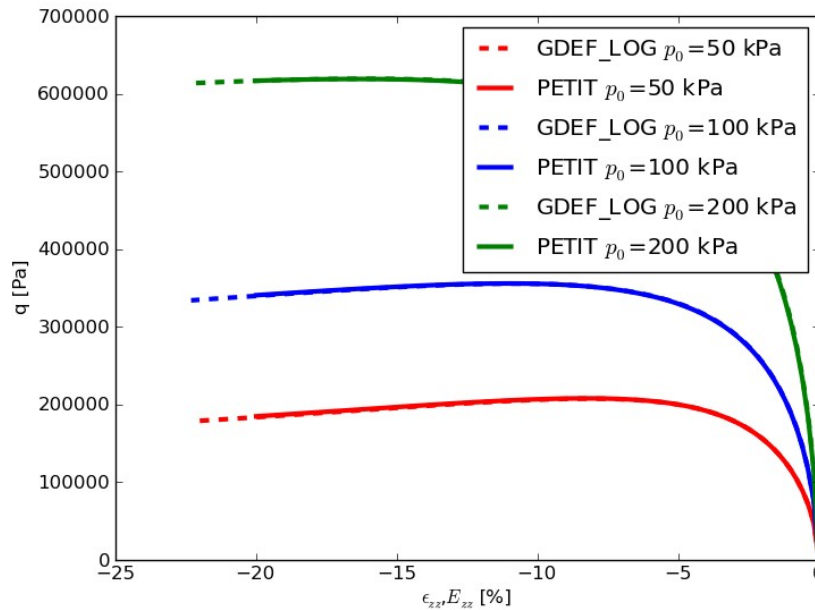


Figure 5 : Equivalent constraint (noted “ Q ”) according to the axial deformation: comparison enters the solutions to small and great deformations Code_Aster, for the pressures of consolidation of 50 , 100 and 200kPa .

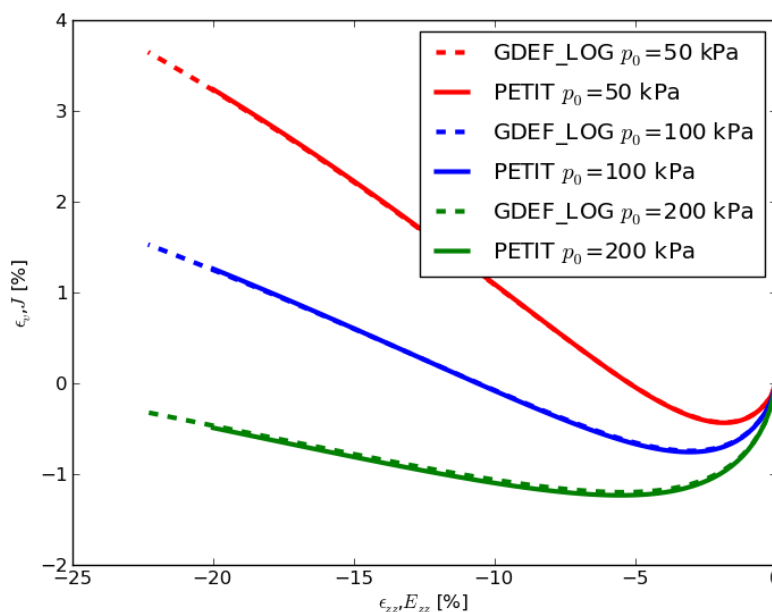


Figure 6 : Total voluminal deformation according to the axial deformation: comparison enters the solutions to small and great deformations Code_Aster, for the pressures of consolidation of 50 , 100 and 200kPa .